Incorporation and Turnover of Biotin-labeled Actin Microinjected into Fibroblastic Cells: An Immunoelectron Microscopic Study

Shigeo Okabe and Nobutaka Hirokawa

Department of Anatomy and Cell Biology, School of Medicine, University of Tokyo, Hongo, Tokyo, 113 Japan

Abstract. We investigated the mechanism of turnover of an actin microfilament system in fibroblastic cells on an electron microscopic level. A new derivative of actin was prepared by labeling muscle actin with biotin. Cultured fibroblastic cells were microinjected with biotinylated actin, and incorporated biotin-actin molecules were detected by immunoelectron microscopy using an anti-biotin antibody and a colloidal gold-labeled secondary antibody. We also analyzed the localization of injected biotin-actin molecules on a molecular level by freeze-drying techniques.

Incorporation of biotin-actin was rapid in motile peripheral regions, such as lamellipodia and microspikes. At ~1 min after injection, biotin-actin molecules were mainly incorporated into the distal part of actin bundles in the microspikes. Heavily labeled actin filaments were also observed at the distal fringe of the densely packed actin networks in the lamellipodium. By 5 min after injection, most actin polymers in microspikes and lamellipodia were labeled uniformly. These findings suggest that actin subunits are added preferentially at the membrane-associated ends of preexisting actin filaments. At earlier times after injection, we often observed that the labeled segments were continuous with unlabeled segments, suggesting the incorporation of new subunits at the ends of preexisting filaments.

Actin incorporation into stress fibers was a slower process. At 2–3 min after injection, microfilaments at the surface of stress fibers incorporated biotin-actin, but filaments in the core region of stress fibers did not. At 5–10 min after injection, increasing density of labeling along stress fibers toward their distal ends was observed. Stress fiber termini are generally associated with focal contacts. There was no rapid nucleation of actin filaments off the membrane of focal contacts and the pattern of actin incorporation at focal contacts was essentially identical to that into distal parts of stress fibers. By 60 min after injection, stress fibers were labeled uniformly. We also analyzed the actin incorporation into polygonal nets of actin bundles. Circular dense foci, where actin bundles radiate, were stable structures, and actin filaments around the foci incorporated biotin-actin the slowest among the actin-containing structures within the injected cells.

These results indicate that the rate and pattern of actin subunit incorporation differ in different regions of the cytoplasm and suggest the possible role of rapid actin polymerization at the leading margin on the protrusive movement of fibroblastic cells.

THE actin microfilament system is a prominent component of the cytoskeleton in a variety of cell types (11, 13, 14, 31, 33). Networks of microfilaments in nonmuscle cells are composed of both actin, the principal structural protein, and a diverse group of regulatory proteins that are collectively known as actin-binding proteins.

There is now increasing evidence suggesting that actin filaments in vivo continue to turn over and change their interaction with each other and with other cell organelles (5). It is known that assembly–disassembly of actin subunits in vitro persists at a steady state and the filament length and interfilament interactions can be altered rapidly by the addition of actin-binding proteins (15, 27). Furthermore, many studies using pharmacological and morphological techniques have suggested that the assembly–disassembly of actin filaments plays some role in dynamic cellular activities and morphogenesis (7, 22, 34, 35). Although these in vitro and in vivo experiments have demonstrated that actin subunits exchange rapidly in areas of highly motile activity, clear descriptions of the underlying molecular mechanism have not yet obtained.

Fibroblastic cells show motile behavior on the culture substratum and have been used as a model of nonmuscle cell motility (1). Actin filaments are organized in a few characteristic patterns in the different cytoplasmic domains of fibroblasts (11, 31). The leading edge contains densely packed actin filaments that are differentially organized in two distinct types of protrusions, microspikes and lamellipodia (11, 33). In microspikes, where the cytoplasm protrudes in the form of long, thin processes, actin filaments form tightly packed bundles. On the other hand, randomly oriented networks of actin filaments fill the cytoplasm of lamellipodia, where the

© The Rockefeller University Press, 0021-9525/89/10/1581/15 $2.00

cell margin forms thin sheet-like extensions. Another prominent actin-containing structure in fibroblastic cells is stress fibers, which are composed of densely packed, large bundles of microfilaments running through the cell body and are associated at their termini with the plasma membrane (6, 10).

Recently, the techniques of microinjection of fluorescently labeled cytoskeletal proteins have been developed and applied to the study of molecular dynamics of actin turnover in fibroblastic cells (2, 8, 16, 17, 36, 37). Microinjection of fluorescently labeled actin has revealed that actin filaments in the leading edge and stress fibers continue to exchange subunits (8, 16). FRAP measurements have also characterized the turnover of actin filaments at a steady state (17, 37). Though these studies have characterized the overall pattern and rate of actin turnover in fibroblasts, they do not have sufficient resolution to determine the sites of subunit addition on a molecular level.

To study the mechanism of actin subunit incorporation on an electron microscopic level, we microinjected biotin-labeled actin into 3T3 fibroblasts and analyzed the pattern of incorporation using an anti-biotin antibody and a secondary antibody conjugated with colloidal gold. Microinjected and antibody-decorated cells were thin sectioned or freeze-dried and observed with an electron microscope. The results indicate that the incorporation of actin subunits occurs at the distal part of actin bundles in microspikes and at the membrane-associated region of actin networks in lamellipodia. We also report that the rate and pattern of actin subunit incorporation differs in four actin-rich cytoplasmic domains: the leading edge, stress fibers, focal contacts, and circular dense foci.

Materials and Methods

Preparation of Biotin-labeled Actin

A new derivative of actin was prepared by labeling skeletal muscle actin with biotin. Actin was prepared from an acetone powder of chicken breast muscle (26). 25 mg of purified G-actin in disassembly buffer (2 mM Tris-HCl, pH 7.5, 0.1 mM $CaCl_2$) was polymerized by the addition of 1 M Tris-HCl, pH 7.5, 0.2 M $MgCl_2$, 3 M KCl, and 100 mM ATP to final concentrations of 10, 2, 100, and 1 mM, respectively. After incubation at 25°C for 10 min, 8 mg of *N*-hydroxysuccinimidyl biotin (at a concentration of 100 mg/ml in DMSO) (18) was added and biotinylation proceeded for 10 min. The reaction was quenched by the addition of 100 mg Na-glutamate, and then F-actin was pelleted for 90 min at 150,000 *g* at 4°C. The pellet was resuspended and depolymerized in 2 ml of disassembly buffer plus 0.5 mM ATP and 0.2 mM DTT. Biotinylated actin preparations were taken through two cycles of polymerization-depolymerization. The final pellet was resuspended in 2 mM Tris-HCl, pH 7.5, and 0.1 mM ATP and dialyzed against the same buffer to obtain G-actin. The sample was clarified by centrifugation at 100,000 *g* for 5 min, frozen in aliquots in liquid nitrogen, and stored at −80°C.

Cell Culture

Mouse 3T3 fibroblasts (a kind gift of H. Yoshikura, University of Tokyo, Tokyo, Japan) were grown at 37°C in DME (Gibco Laboratories, Grand Island, NY) supplemented with 5% FCS (Gibco Laboratories). For microinjection studies, the cells were trypsinized and plated onto glass coverslips for immunofluorescence: 35-mm petri dishes for immunoelectron microscopy of thin-sectioned cells and small fragments of coverslips for freeze-drying. The cells were allowed to settle for 24 h before microinjection.

Microinjection

Microinjection was performed on an inverted microscope (Diaphot; Nikon Inc., Garden City, NY) equipped with a micromanipulator (Narishige Scientific Laboratory, Tokyo, Japan) and a stage heater. Procedures for microinjection (24) were similar to that described by Graessmann et al. (9). Biotin-actin was diluted to 2 mg/ml, clarified by centrifugation, and loaded into needles. Cells were penetrated by the needles at the perinuclear region.

Immunofluorescence

Cells were briefly washed in PHEM buffer (60 mM Pipes, 25 mM Hepes, 10 mM EGTA, and 2 mM $MgCl_2$, pH 6.9), lysed with PHEM buffer plus 0.3% Triton X-100 and 10 μM Taxol for 2 min, and fixed with 0.3% glutaraldehyde in PHEM buffer for 20 min. After fixation, cells were washed with PBS, incubated with a solution of PBS plus 1% Triton X-100 for 20 min at room temperature, and then placed in PBS with 1 mg/ml $NaBH_4$ for 10 min to quench the glutaraldehyde. The samples were briefly washed with PBS and incubated successively with the following antibodies: rabbit anti-biotin (Enzo Biochem, Inc., New York, NY), fluorescein-conjugated goat anti-rabbit IgG, and fluorescein-conjugated rabbit anti-goat IgG. All antibodies were diluted 1:100 in PBS. Fluorescein-conjugated second antibodies were from Cappel Laboratories (Cochranville, PA). After each incubation, the cells were washed three times for 10 min in PBS plus 0.1% Triton X-100. The samples were further reacted with 0.2 μM rhodamine-phalloidin in PBS (Molecular Probes Inc., Eugene, OR), washed three times for 5 min in PBS, mounted on slides, and examined with a microscope (Axiophot; Carl Zeiss, Inc., Thornwood, NY).

Immunocytochemistry for Electron Microscopy

The extraction and fixation procedures were the same as that for immunofluorescence except that 0.5% glutaraldehyde was used for fixation. The fixed cells were briefly washed with TBS, pH 7.4, treated with TBS plus 0.2% Triton X-100 for 30 min, and then reacted with 1 mg/ml $NaBH_4$ in TBS for 10 min. They were incubated with 10% goat serum in TBS, pH 7.4, for 30 min to block nonspecific reactions and, subsequently, with rabbit anti-biotin diluted 1:100 in TBS plus 1% BSA for 3 h. The cells were washed twice for 10 min in TBS, pH 7.4, and then three times for 10 min in TBS, pH 8.2. The secondary antibody (goat anti-rabbit IgG) coupled to 5-nm gold (Janssen Pharmaceutica, Beerse, Belgium) was diluted 1:10 in TBS plus 1% BSA and the reaction was continued for a total of 12 h at room temperature and/or at 4°C. After washing five times for 10 min in TBS, pH 8.2, the cells were postfixed in 1% glutaraldehyde plus 0.2% tannic acid in 0.1 M phosphate buffer, pH 7.2, for 30 min (20), washed in the same buffer, postfixed in 0.5% osmium tetroxide at 4°C for 10 min, and washed extensively with distilled water. Injected cells were identified by using the video tape recorder during the injection procedure and marked by a needle or an objective marker. The marks on the substrate were used as a reference for embedding and sectioning.

Embedding and Sectioning for Electron Microscopy

Postfixed samples were stained in 1% uranyl acetate for 30 min, dehydrated, and embedded in Epon 812. Epon-embedded samples were excised and serially sectioned as previously described (24, 25).

Preparation of Freeze-dried Samples

For native cells, the samples were extracted in the same way as for immunofluorescence and fixed with 1% glutaraldehyde in PHEM buffer for 30 min. The fixed cells were washed with 0.1 M phosphate buffer, pH 7.2, and treated with 1% glutaraldehyde plus 0.2% tannic acid in the same buffer for 30 min. After washing with the same buffer, cells were postfixed in 0.5% osmium tetroxide at 4°C for 10 min and washed extensively with distilled water.

For cells injected with biotin-actin, the procedures for extraction, fixation, antibody decoration, and postfixation were the same as described in immunocytochemistry for electron microscopy. Postfixed samples were rinsed in 70% methanol in water. Freezing was performed as described previously (12). The frozen cytoskeletons were transferred into the freeze-fracture device (Balzers Corp., Hudson, NH), warmed up to −90°C at a vacuum of 10^{-6} torr for 2 h, and rotary shadowed with platinum-carbon (11, 12). The resulting platinum replica was treated with 25% hydrofluoric acid to remove the coverglass, and then with household bleach, washed with distilled water, and picked up on a formbar-coated grid.

Electron Microscopy

Samples were observed with an electron microscope (1,200 EX; JEOL

USA, Peabody, MA) at 80 kV for thin sections and at 100 kV for platinum replicas.

Other Methods

Biotin-labeled BSA was prepared as follows. 25 mg of BSA in 10 mM Tris-HCl, pH 7.5, was reacted with 8 mg of *N*-hydroxy-succinimidyl biotin for 30 min at 25°C, and the reaction was stopped by the addition of 100 mg of Na-glutamate. BSA and unbound biotin were separated on a Sephadex G-25 column, and biotin-BSA-containing fractions were collected and concentrated by precipitation with 50% saturated ammonium sulfate. The pellet of ammonium sulfate precipitation was dissolved in 2 mM Tris-HCl, pH 7.5.

SDS-gel electrophoresis was performed according to the method of Laemmli using 10% acrylamide in the running gel and 5% acrylamide in the stacking gel (19). Protein concentrations were estimated by the method of Bradford (3).

Results

Characterization of Biotin-labeled Actin

We prepared chicken muscle actin labeled with biotin as a probe for actin filament dynamics in fibroblastic cells. As shown in Fig. 1, this preparation was essentially free of contaminants, such as myosin and tropomyosin. The labeled actin formed 7-nm filaments that were indistinguishable from native actin filaments (data not shown). Fig. 2 shows time course of biotin-actin polymerization in vitro. Although the extent of polymerization of biotin-actin was somewhat smaller than that of unlabeled actin (~90%), the rate and pattern of polymerization were almost identical. We also estimated critical concentration of biotin-actin by using the plot of specific viscosity vs. actin concentration. The estimated critical concentration did not differ between biotinylated and unlabeled actin preparations (data not shown). When injected into 3T3 fibroblasts, biotin-actin was rapidly incorporated into the cytoskeleton. Fig. 3, *a* and *b*, shows a cell permeabilized 2 min 27 s after injection. Anti-biotin staining was prominent in peripheral regions corresponding to ruffling membranes (Fig. 3 *b*, *arrows*). Although bright patches of fluorescence were observed in the interior cellular regions, incorporation of biotin-actin into stress fibers was not significant at this time point (Fig. 3 *b*, *arrowheads*). Anti-biotin staining in stress fibers initially appeared 5 min after injection and by 30 min it became prominent in a majority of injected cells. Fig. 3, *c* and *d*, shows a cell permeabilized 3 h after injection, and biotin-actin was incorporated into stress fibers homogeneously. Intense staining with anti-biotin was observed in the cells incubated for >24 h and this suggests that extensive degradation of biotin-actin does not occur in vivo. The observed pattern and time course of biotin-actin incorporation is in good agreement with those of previous studies using fluorescent analogues of actin (8, 16). These in vitro and in vivo experiments collectively indicate that biotin-labeled actin can be used as a probe for actin filament turnover within living cells.

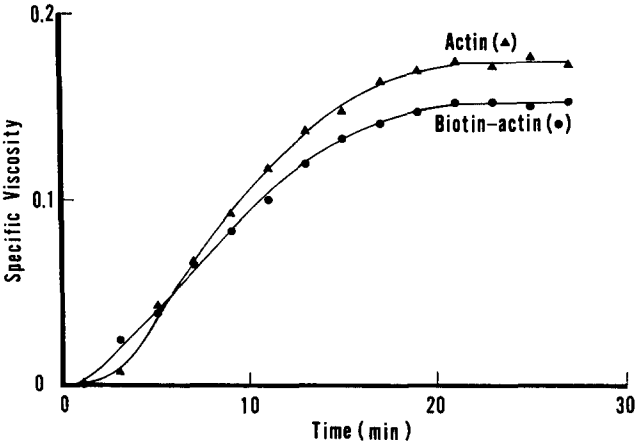

Figure 2. Polymerization of biotin-actin and unlabeled actin as monitored by viscosity measurements. Monomeric actin (0.15 mg/ml) was polymerized by the addition of (final concentrations) 50 mM KCl and 1 mM $MgCl_2$.

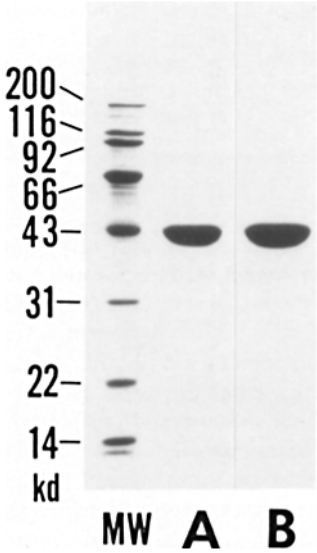

Figure 1. SDS-PAGE analysis of the preparation of actin modified with biotin. Actin prepared from chicken breast muscle (lane *A*) was labeled with biotin and purified through two cycles of polymerization-depolymerization. Only a single band which had the same electrophoretic mobility with actin (43 kD) was observed in the final product (lane *B*). *MW*, molecular mass standards.

Controls

We studied the incorporation of biotin-actin microinjected into fibroblastic cells on an electron microscopic level using an anti-biotin antibody and a goat anti-rabbit IgG antibody conjugated with colloidal gold. To critically interpret patterns of colloidal gold distribution in microinjected cells, it was important to ascertain the level of the nonspecific binding of antibodies and colloidal gold to the cytoskeleton of 3T3 fibroblasts. Fig. 4 shows two characteristic actin-containing structures, a lamellipodium and a dense focus of actin bundles, in uninjected cells. Few gold particles were observed in these areas and this indicates that the nonspecific binding of primary and secondary antibodies is negligible.

To eliminate the possibility of nonspecific binding of biotinylated proteins to the cytoskeleton, we microinjected biotin-labeled BSA into 3T3 fibroblasts. Fig. 5 shows a cell injected with biotin-labeled BSA, permeabilized, and fixed 15 min after injection. Anti-biotin staining of the cytoplasm is very low and this result indicates that biotinylated proteins do not adhere nonspecifically to the cytoskeleton.

Actin Turnover in the Leading Edge

The incorporation of biotin-actin into actin networks of the leading edge was studied by immunoelectron microscopy. We recorded the morphology of injected cells on a videotape and analyzed the motile behavior of the leading edge until

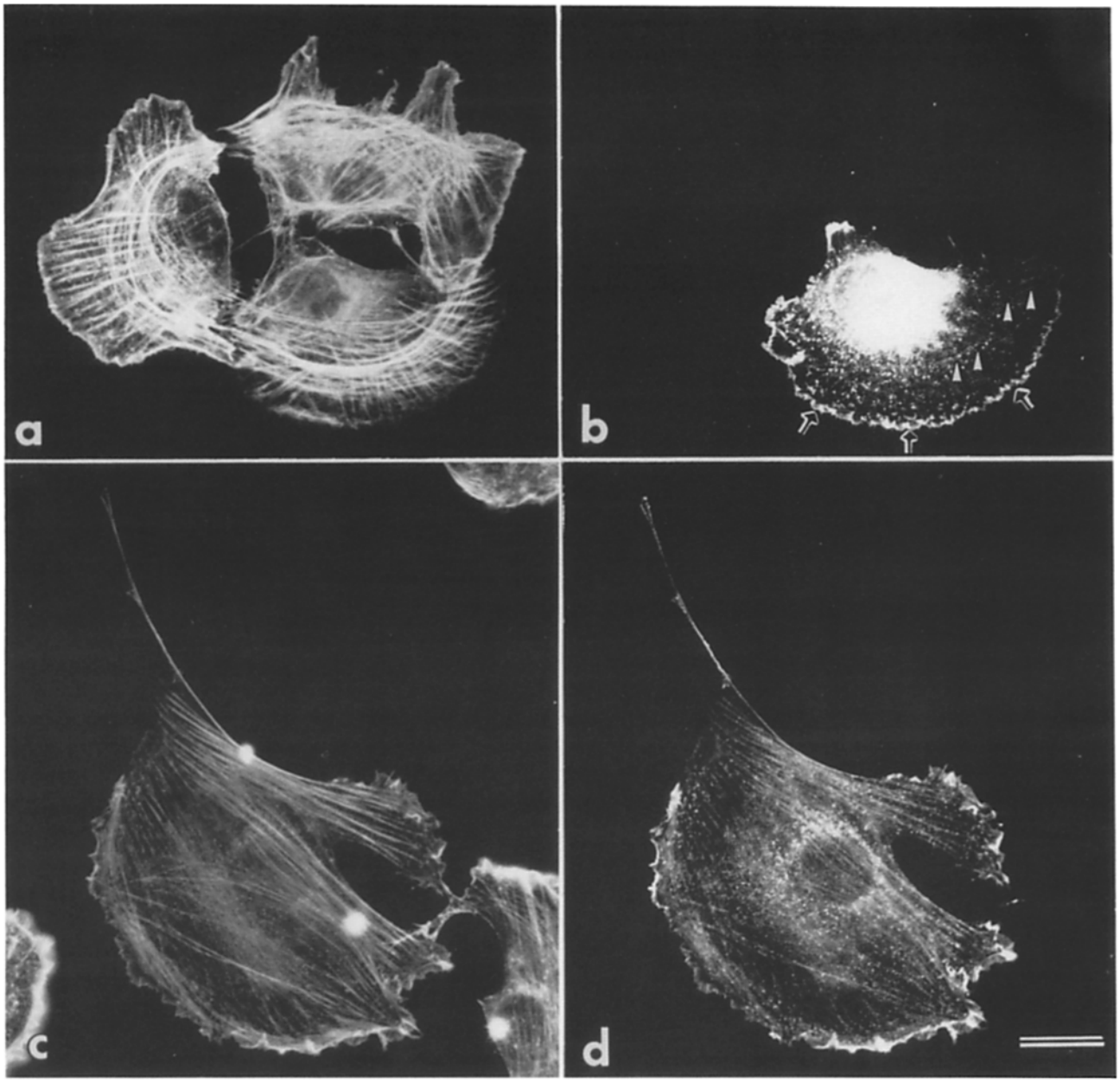

Figure 3. 3T3 fibroblastic cells microinjected with biotin-actin, permeabilized and fixed, and then stained with an anti-biotin antibody and rhodamine-phalloidin. (*a*) Rhodamine-phalloidin staining showing total F-actin distribution of a cell permeabilized 2 min 27 s after injection. (*b*) Fluorescein anti-biotin staining of the same cell as in *a* showing polymerized biotin-actin after injection. Intense fluorescence was observed in ruffling membrane (*arrows*), but stress fibers were not stained prominently (*arrowheads*). (*c*) Rhodamine-phalloidin staining of a cell permeabilized 3 h after injection. (*d*) Anti-biotin staining of the same cell as in *c*. Biotin-actin was incorporated into stress fibers homogeneously. Bar, 20 μm.

cells were permeabilized and fixed. Cells that showed no change in the shape of the leading edge and its activity were processed further. Under our culture conditions, there was little net translocation of the leading edge of 3T3 fibroblasts during observations. Fig. 6 *a* shows a bundle of actin filaments in a microspike of a cell injected 52 s before permeabilization. Biotin-actin assembled after injection was recognized by an antibody to biotin and colloidal gold, and gold particles were localized in the distal part of actin bundles (*arrows*). At 5 min after injection, the proximal part of actin bundles also incorporated biotin-actin (Fig. 6 *b*). The core of actin bundles tended to be labeled less prominently than the surface at this time point (*arrowheads*). This was not due to the limited penetration of antibodies and/or colloidal gold because colloidal gold adhered to the core region of actin bundles in microspikes of a cell incubated for 1 h after injection (Fig. 6 *c*). These results indicate that the turnover of actin filaments is rapid both at the distal end and peripheral, membrane-associated regions of microspikes and suggest that the incorporation of monomeric actin occurs at the membrane-associated ends of preexisting actin filaments in microspikes.

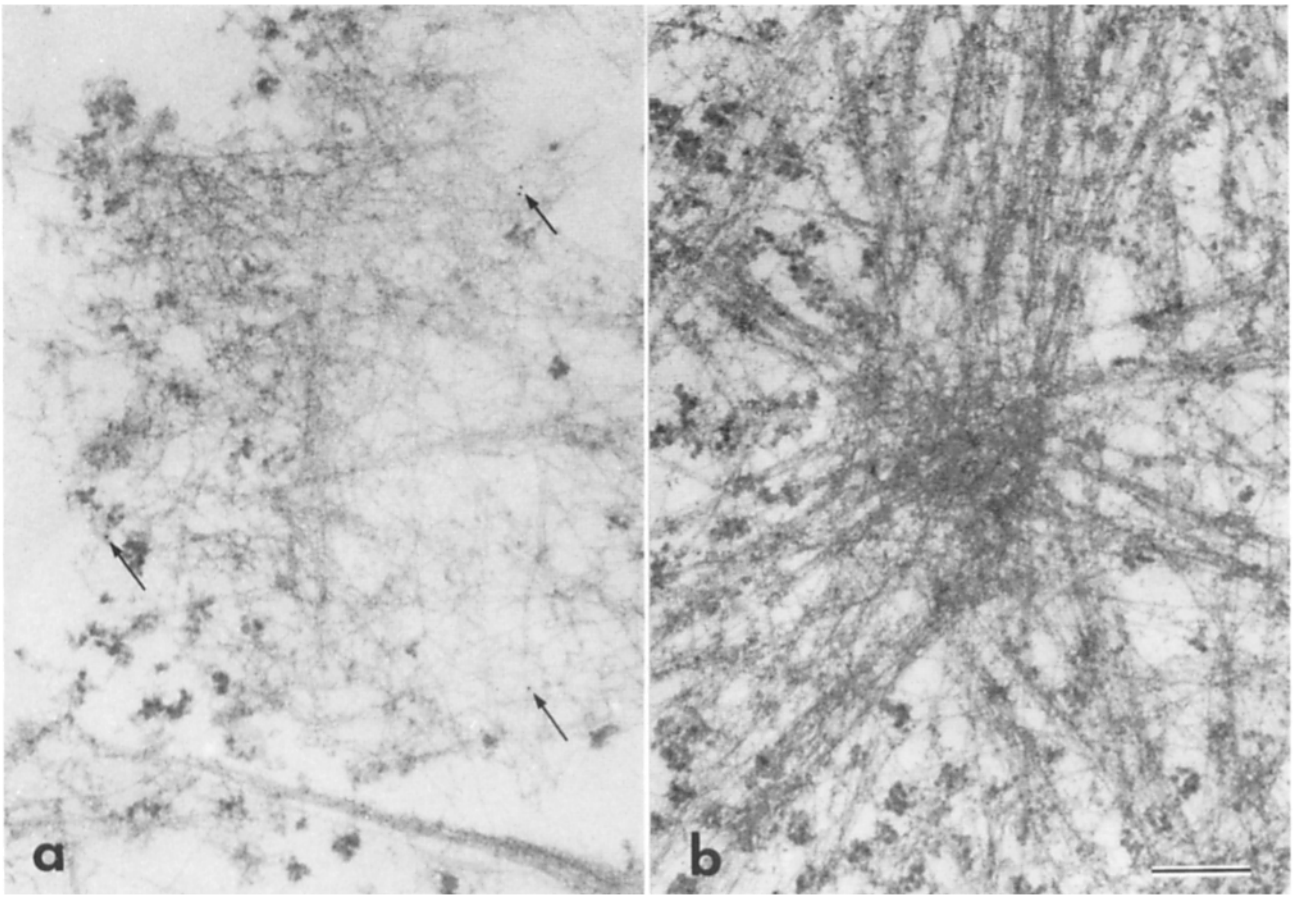

Figure 4. Thin sections of 3T3 fibroblastic cells that were not injected with biotin-actin and processed in an identical way as immunoelectron microscopy for injected cells. (*a*) A lamellipodium of a control cell. The nonspecific background staining is extremely low (*arrows*). (*b*) A focus of polygonal networks of actin bundles in another control cell. Few gold particles were observed in this region. Bar, 200 nm.

We also examined the actin dynamics in lamellipodia. Fig. 7 *a* shows a thin-section electron micrograph of a lamellipodium of the cell injected 2 min 32 s before permeabilization. Dense networks and bundles of actin filaments were observed, and gold particles were mainly localized to the membrane-associated fringe of actin filament networks. A microfilament bundle running perpendicularly to the cell margin incorporated biotin-actin into its distal part (*arrows*). By 5 min after injection, actin filaments in lamellipodia were labeled homogeneously (Fig. 7 *b*). No substantial changes of the distribution of colloidal gold were observed at 1 h after injection (data not shown). These results indicate that the incorporation of monomeric actin mainly occurs at the membrane-associated distal fringe of the actin network in lamellipodia and the turnover of actin filaments occurs in a centripetal fashion.

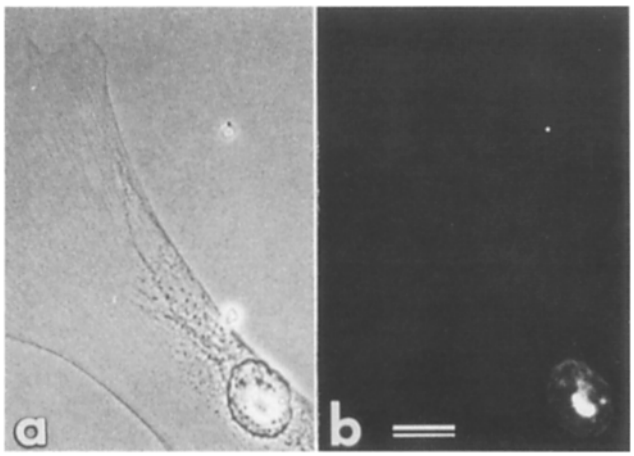

Figure 5. A 3T3 fibroblast microinjected with biotin-labeled BSA at 2 mg/ml and stained with an anti-biotin antibody. (*a*) Phase-contrast image of a cell permeabilized 15 min after injection with biotin-labeled BSA. (*b*) Fluorescein anti-biotin staining of the same cell as in *a*. Bar, 20 μm.

Actin Turnover in Stress Fibers

When cells were permeabilized and fixed within 1 min after injection, most stress fibers contained no gold particles (data not shown). Fig. 8 shows stress fibers of a cell injected with biotin-actin 2 min 32 s before permeabilization. Thick stress fibers were still largely unlabeled, but some gold particles were localized on the surface of these fibers (*arrows*). At 5 min after injection, increasing density of colloidal gold along stress fibers toward their peripheral ends was observed. The distal ends of stress fibers usually spread out to become thinner diameter bundles in the peripheral cellular regions and were labeled with anti-biotin prominently at this time point (Fig. 9 *a*). In contrast, the middle part of the same stress

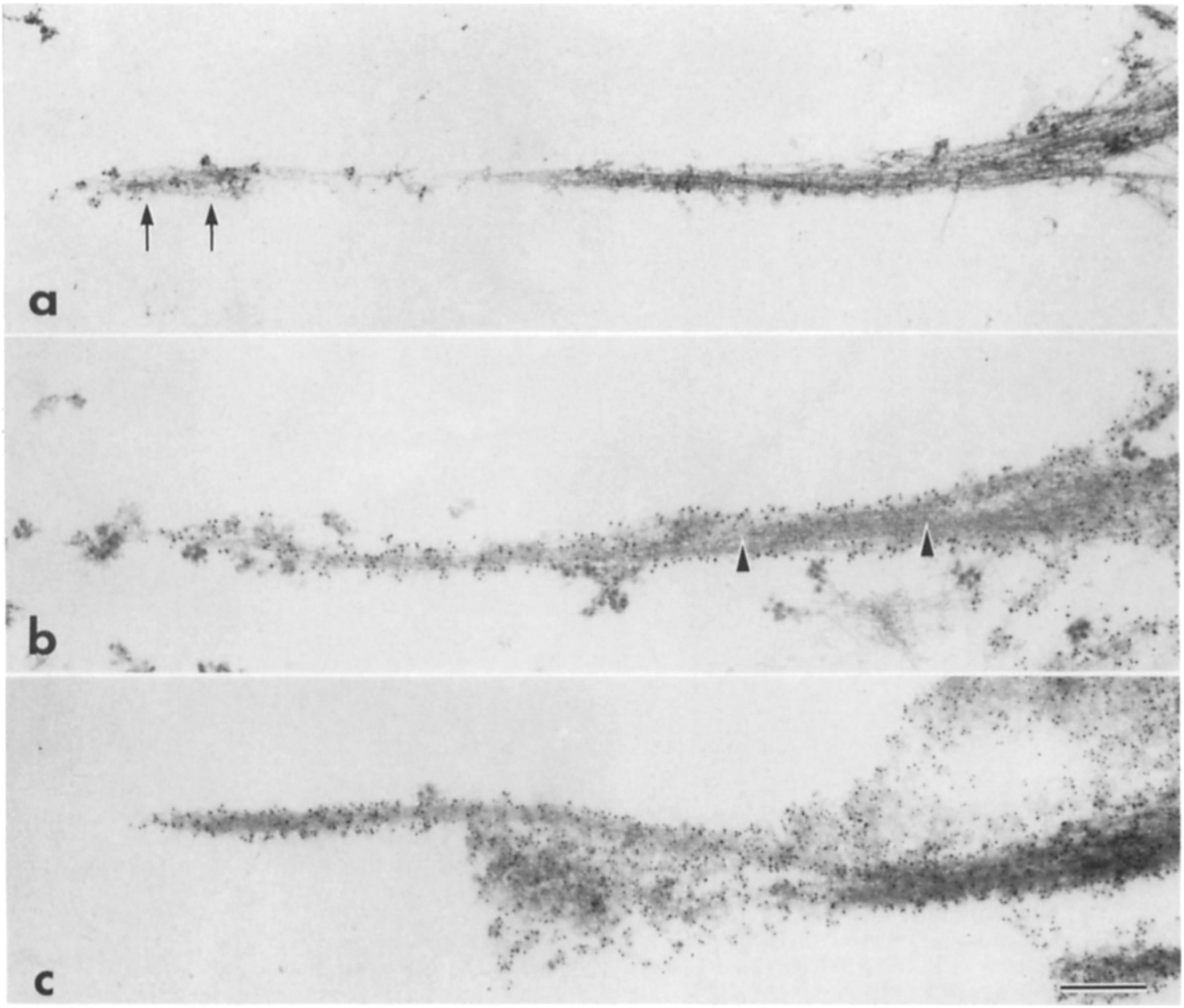

Figure 6. Time course of biotin-actin incorporation into actin bundles of microspikes. (*a*) A microspike of a cell permeabilized 52 s after injection. Labeled actin subunits polymerized after injection were recognized by an antibody to biotin and colloidal gold. Gold particles were localized in the distal part of actin bundles (*arrows*). (*b*) Localization of biotin-actin within a microspike of a cell incubated for 5 min 2 s after microinjection. The proximal part of the actin bundle incorporated biotin-actin, but the core region was labeled less prominently (*arrowheads*). (*c*) A microspike of a cell injected with biotin-actin 1 h before permeabilization. Homogeneous labeling of the actin bundle with colloidal gold was observed. Bar, 200 nm.

fibers, which passed through the perinuclear region, contained less gold particles (Fig. 9 *b*). This increasing density of labeling along stress fibers was frequently observed by 10 min after injection. As incubation time lengthened, the labeling density of stress fibers became uniform. Fig. 10 shows thick diameter bundles in the perinuclear region of a cell incubated for 1 h after injection. Large actin bundles contained gold particles homogeneously and the labeling density did not differ between the surface and core regions. One possible explanation for the increasing density of labeling along stress fibers is that thinner parts of fibers in peripheral cellular regions incorporate biotin-actin more rapidly than thicker parts in the perinuclear region. Another possibility is that the rate of actin incorporation at the surfaces of fibers is uniform along their length but the increase of surface area as the diameter of stress fibers decrease results in a relative increase of labeling density per unit area of thin-sectioned cells.

To approach this question, we analyzed the cytoskeletons of 3T3 fibroblasts that were injected with biotin-actin, decorated with antibodies and colloidal gold, freeze-dried, and rotary shadowed with platinum-carbon. Fig. 11 shows stress fibers of a native 3T3 fibroblast. Three-dimensional organization of densely packed actin filaments in parallel running stress fibers were clearly observed. We attempted to see the distribution of biotin-actin shortly after injection. To do this, cells grown on fragments of coverglass were injected rapidly (within 5 min) and permeabilized and fixed immediately after injection. We did not determine the exact incubation time for each cell. In replicas, nonspecific labeling of uninjected cells was quite low and it was not difficult to identify the in-

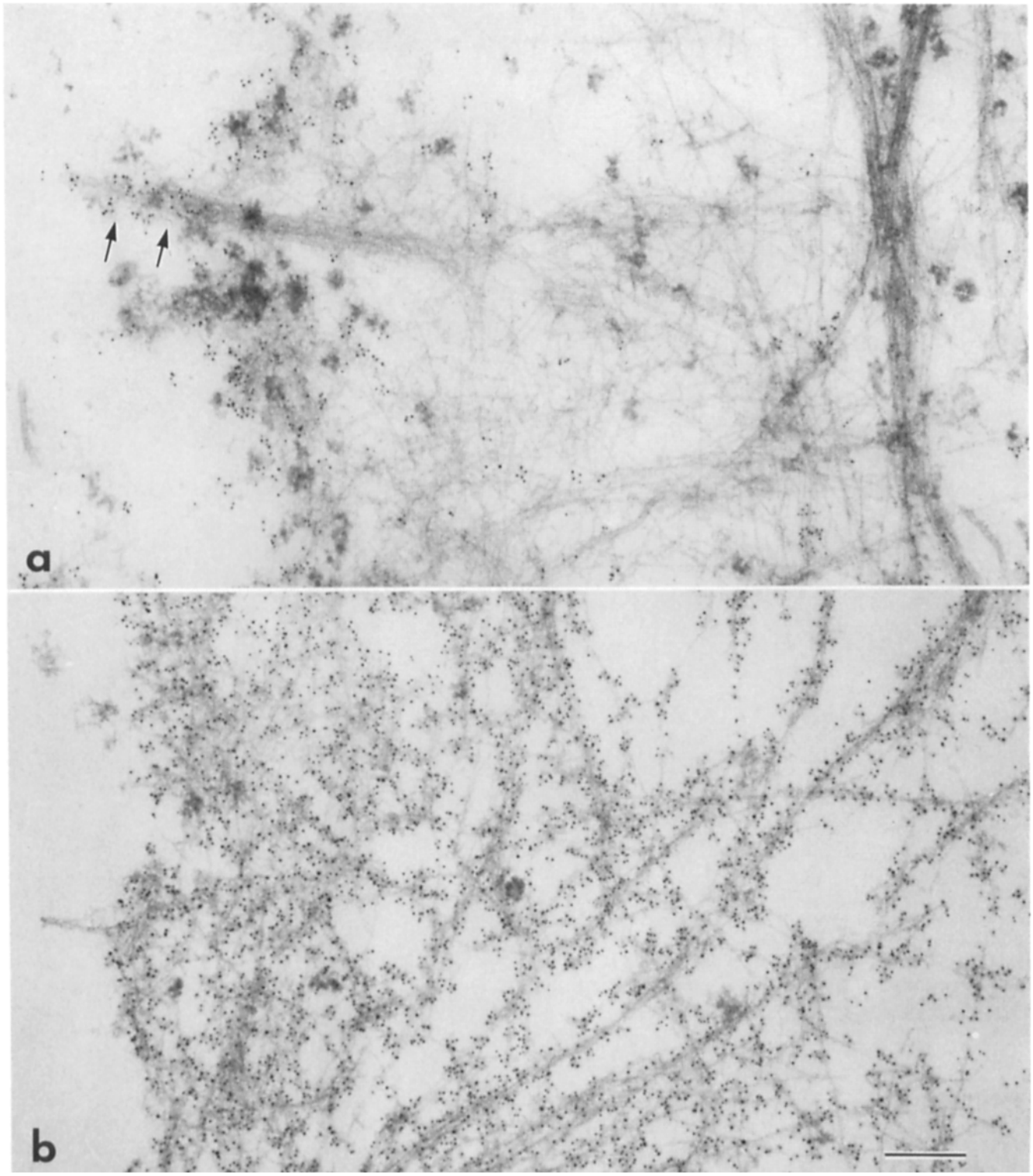

Figure 7. Time course of biotin-actin incorporation into actin networks of lamellipodia. (*a*) A lamellipodium of a cell permeabilized 2 min 32 s after injection. Gold particles were mainly localized to the membrane-associated, distal margin of actin networks. A microfilament bundle, which was embedded in dense meshwork of actin filaments, also incorporated biotin-actin into its distal part (*arrows*). (*b*) Actin filament networks in a lamellipodium of a cell incubated for 5 min after injection. Actin filaments in the lamellipodium were labeled homogeneously. Bar, 200 nm.

jected cells because of the high density of colloidal gold particles on the filaments. Fig. 12 *a* illustrates the distribution of colloidal gold on the surface of thick stress fibers. Although complexes of antibodies and colloidal gold were localized on the stress fibers (*arrows*), the labeling density of thick stress fibers in the perinuclear region was not high and bare surfaces of fibers were frequently observed (*arrowheads*). In contrast, thin actin bundles in the peripheral cel-

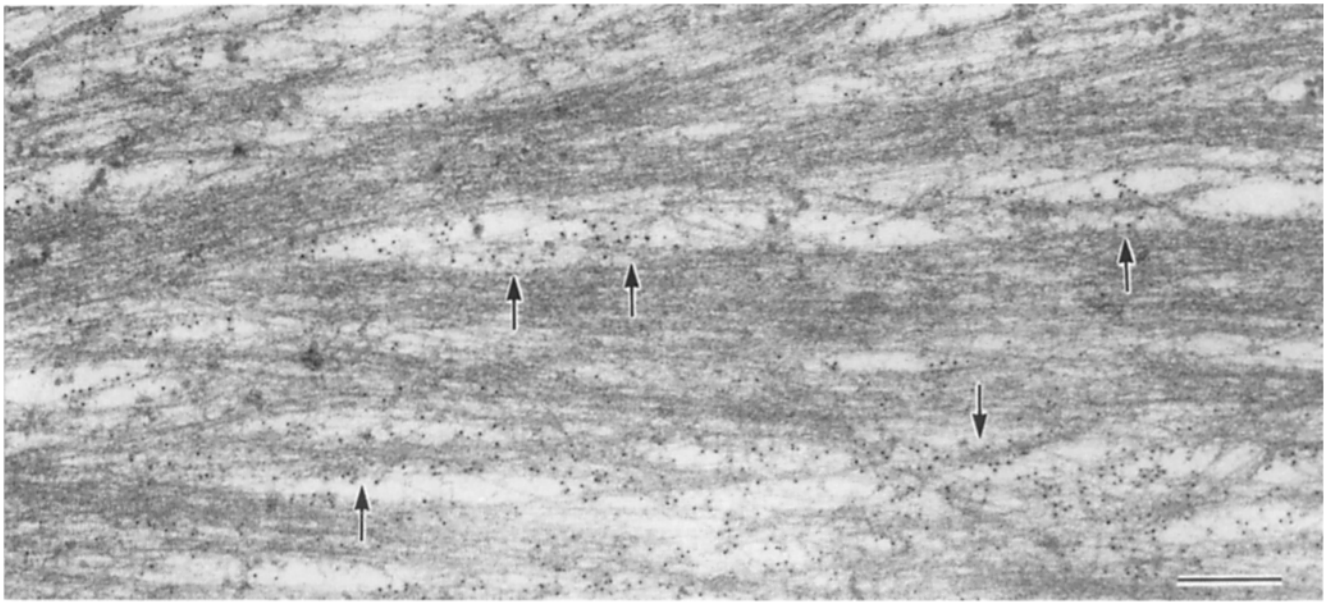

Figure 8. An electron micrograph of stress fibers within a cell injected with biotin-actin 2 min 32 s before permeabilization. Gold particles were localized on the surface of actin bundles. (*arrows*). Bar, 200 nm.

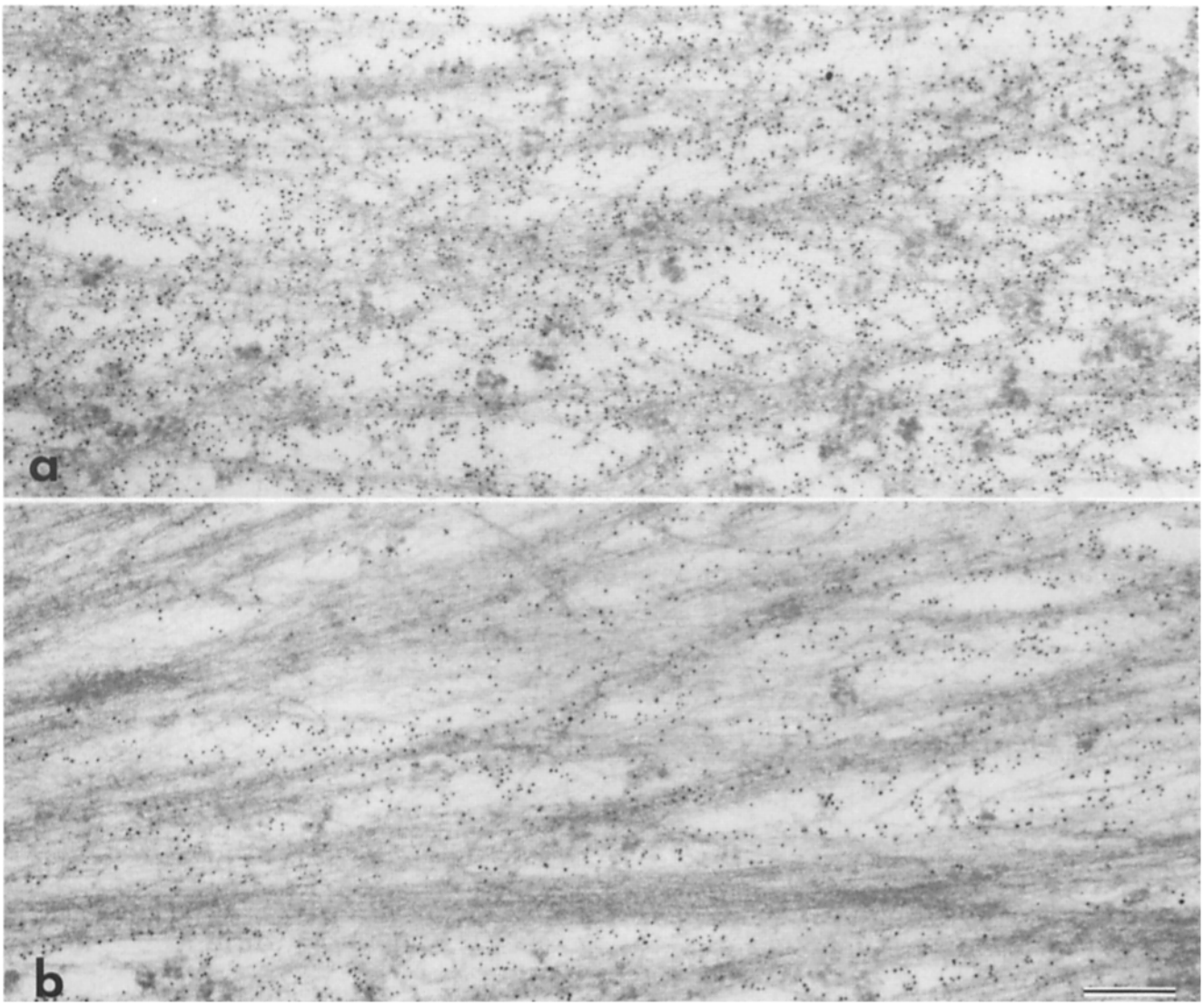

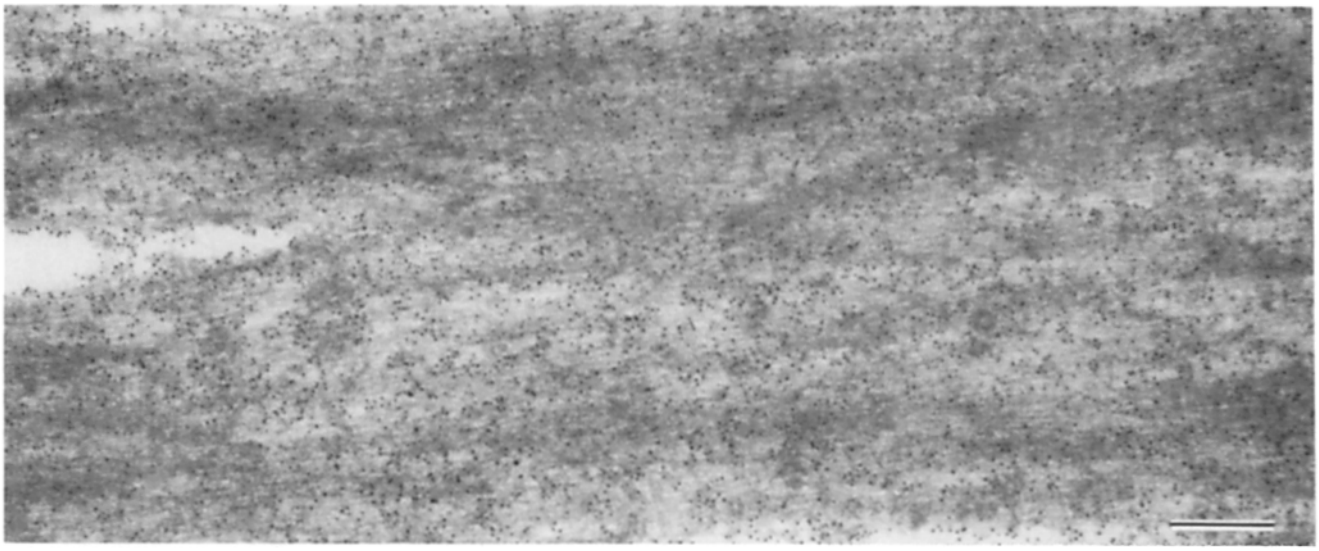

Figure 10. Thick stress fibers running in the perinuclear region of a cell incubated for 1 h after injection. Large actin bundles contained gold particles homogeneously. Bar, 200 nm.

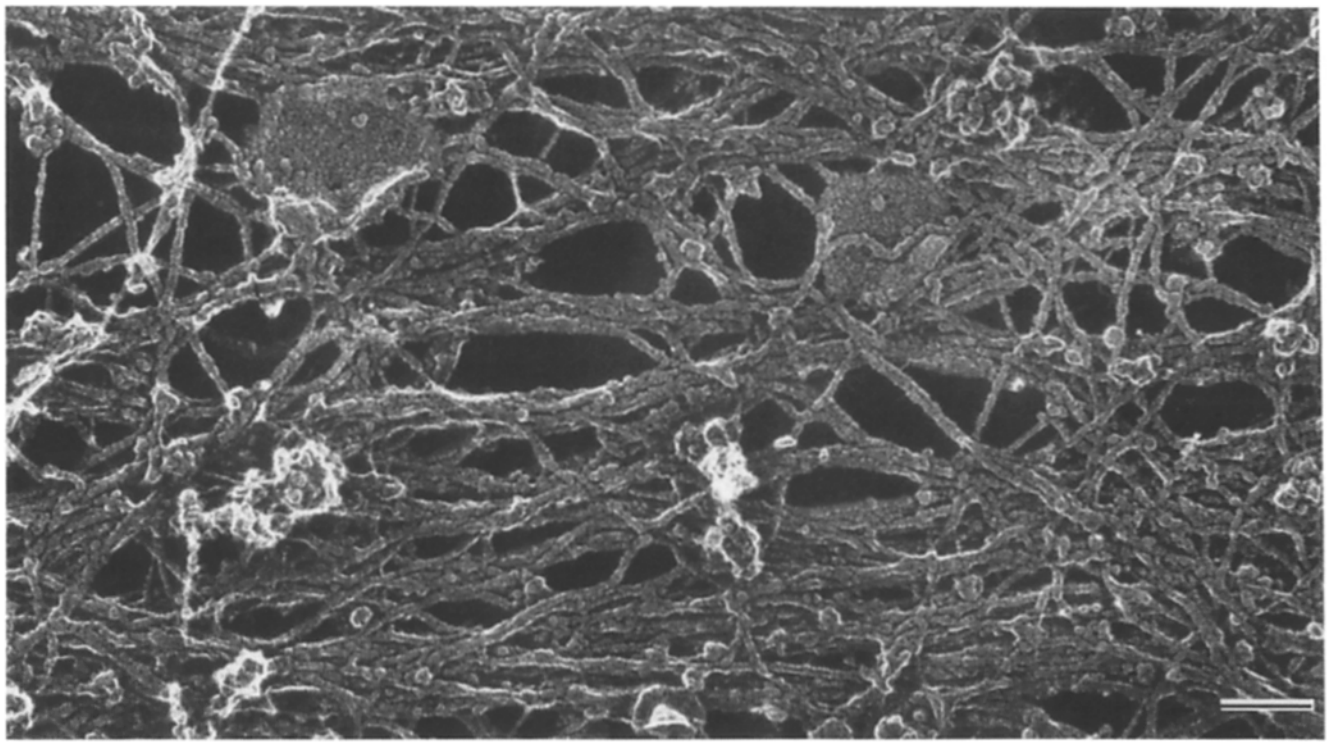

Figure 11. Rapidly frozen, freeze-dried cytoskeleton of stress fibers in a native 3T3 fibroblast. Single actin filaments, which were densely packed within parallel running stress fibers, were clearly observed. Bar, 100 nm.

Figure 9. Increasing density of labeling along stress fibers toward their peripheral ends within a cell injected with biotin-actin 5 min 2 s before permeabilization. (*a*) The peripheral part of stress fibers spreading out to become thinner diameter bundles. These thinner bundles incorporated biotin-actin prominently. (*b*) The middle part of the same stress fibers as in *a* passing through the perinuclear region. The stress fibers became thick in this part and contained less gold particles. Bar, 200 nm.

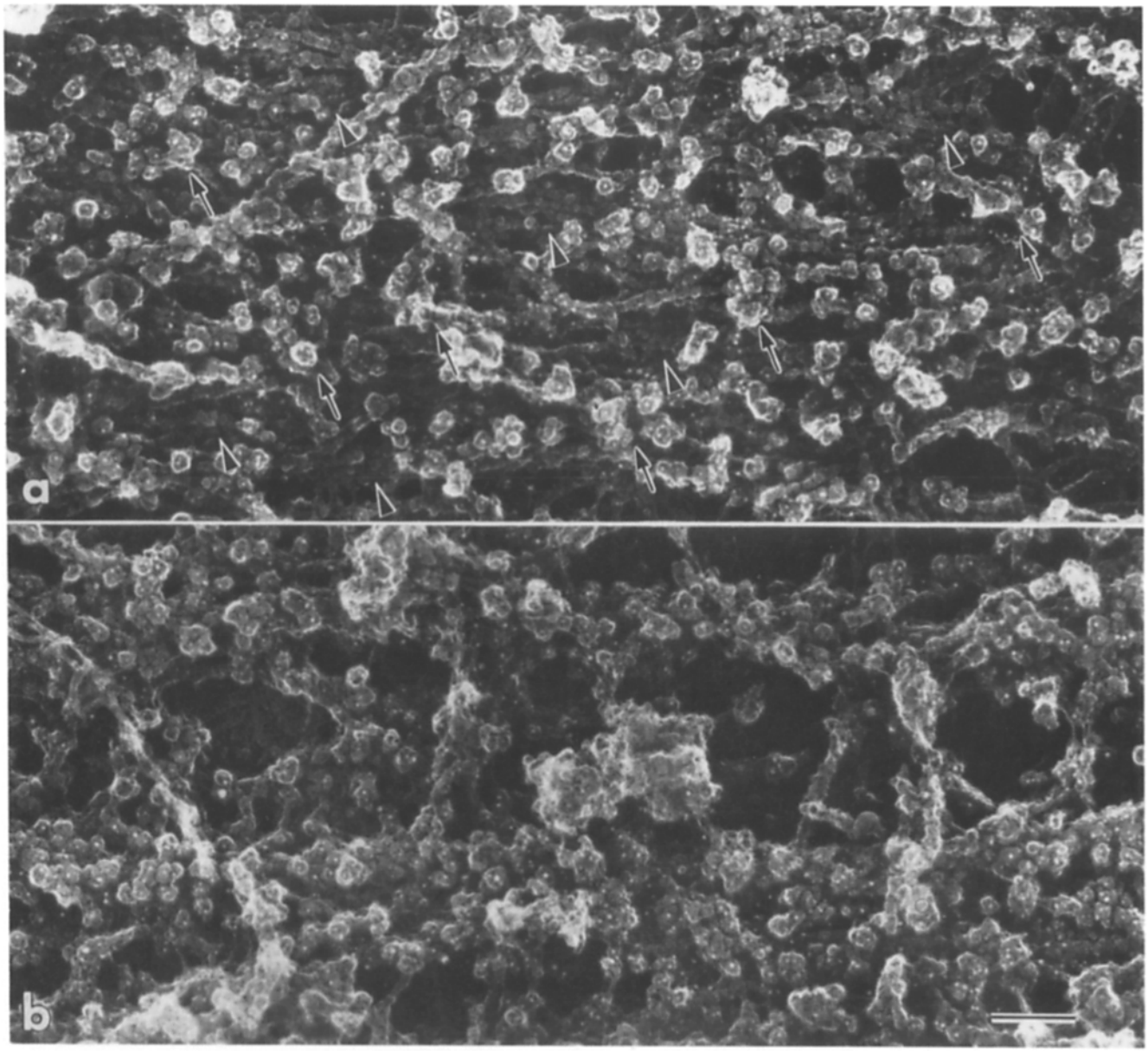

Figure 12. Replica of a freeze-dried cytoskeleton of a cell permeabilized and fixed shortly (<5 min) after injection and decorated with an anti-biotin antibody and colloidal gold. (*a*) The distribution of colloidal gold on the surface of thick stress fibers in the perinuclear region. Complexes of antibodies and colloidal gold were localized on the stress fibers (*arrows*) but bare surfaces of stress fibers were frequently observed (*arrowheads*), suggesting that the labeling density was not high. (*b*) Thin stress fibers fully decorated with complexes of antibodies and colloidal gold in the peripheral regions of the same cell as in *a*. The decoration with antibodies and colloidal gold completely masked the surfaces of stress fibers. Bar, 100 nm.

lular regions of the same cell were fully decorated with complexes of antibodies and colloidal gold along their length, and the native appearance of each fiber was mostly masked by these complexes (Fig. 12 *b*). These results indicate that the rate of actin incorporation at the surfaces of stress fibers really differs at different parts of stress fibers. In both thin-sectioned and freeze-dried cytoskeletons, we could not detect any periodic localization of colloidal gold along stress fibers, which was previously reported by Amato and Taylor (2). In summary, these results illustrate that the incorporation of actin into stress fibers is a slower process and occurs more rapidly in thinner fibers at the cellular periphery.

Actin Turnover at Focal Contacts

Focal contacts are sites of cell-substratum adhesion and the ends of stress fibers are generally anchored at these regions. We first analyzed the overall pattern of actin incorporation into focal contacts by using immunofluorescence microscopy in combination with interference reflection microscopy (10). When injected cells were permeabilized within 5 min after injection, no detectable staining with anti-biotin was observed at focal contacts. Incubation of injected cells for ~10 min resulted in the appearance of intensely stained streaks in the peripheral cellular regions (Fig. 13, *b* and *d*). These streaks were located at the termini of stress fibers (Fig. 13

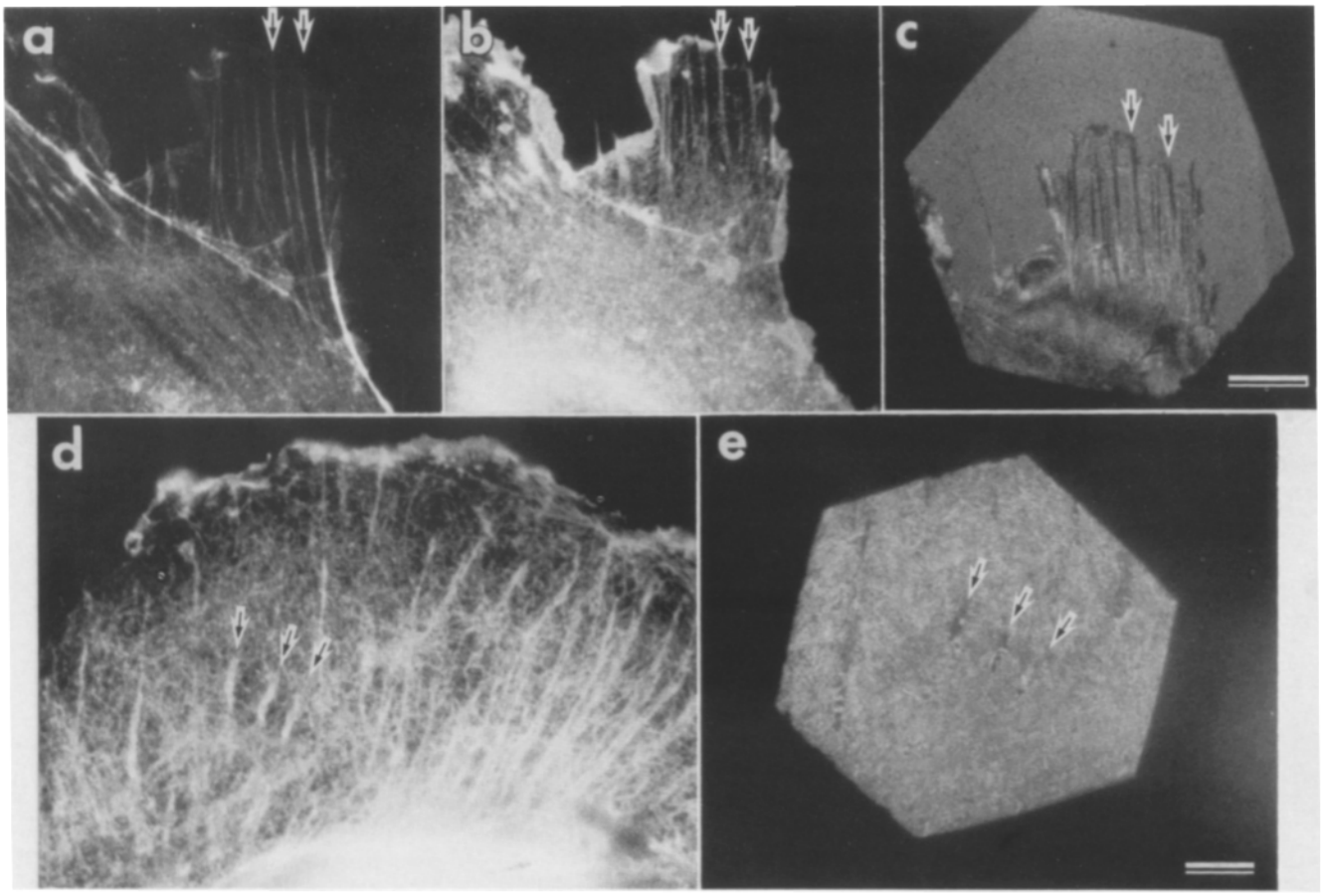

Figure 13. Fluorescence and interference reflection images of cells injected with biotin-actin and stained with an anti-biotin antibody. (*a*) Rhodamine-phalloidin staining of a cell injected 11 min 38 s before permeabilization. (*b*) Fluorescein anti-biotin staining of the same cell as in *a*. Brightly stained streaks correspond to the termini of stress fibers shown in *a* (*arrows*). (*c*) The interference reflection microscopic image shows that brightly stained streaks also correspond to focal contacts (*arrows*). (*d*) Fluorescein anti-biotin staining of another cell incubated for 9 min 22 s after injection. Intensely stained streaks were observed inside the cell (*arrows*). (*e*) The interference reflection microscopic image of the same cell as in *d*, indicating that bright streaks correspond to focal contacts (*arrows*). Bars, 10 μm.

a) and interference reflection microscopy revealed that they also corresponded to the areas of focal contacts (Fig. 13, *c* and *e*). In cells permeabilized >30 min after injection, anti-biotin staining in stress fibers became prominent and focal contacts were no longer detected as discrete fluorescent patches. Although the appearance of intensely stained streaks might be due to rapid turnover of actin filaments at the distal part of stress fibers, it is also possible that the appearance of anti-biotin staining at focal contacts reflects extensive polymerization of actin filaments at these specialized membrane domains. To distinguish these two possibilities, we further analyzed incorporation of biotin-actin at focal contacts by using immunoelectron microscopy. If focal contacts serve as polymerization sites of monomeric actin, extensive formation of microfilaments would be observed immediately after injection. Fig. 14 *a* shows a focal contact in the cell injected with biotin-actin and permeabilized 2 min 32 s after injection. A microfilament bundle closely associated with extracellular matrix (Fig. 14 *a*, *arrows*) was largely unlabeled, suggesting that focal contacts do not work as the sites of rapid nucleation of new filaments in vivo. When cells were incubated for 5–10 min after injection, actin bundles at focal contacts had already incorporated biotin-actin (Fig. 14 *b*). The rate and pattern of actin incorporation at focal contacts appeared to be almost identical to those in the distal part of stress fibers.

Actin Turnover in the Foci of Polygonal Network

Polygonal nets of actin bundles were frequently observed in 3T3 fibroblasts and were composed of circular dense foci and actin bundles interconnecting them. Fig. 15 *a* shows one of the foci within a cell injected 2 min 32 s before permeabilization. No gold particles were localized on the core region and radiating filaments. The foci remained largely unlabeled until 5 min after injection and then gradually incorporated biotin-actin. At 1 h after injection, prominent incorporation of biotin-actin into the foci was observed (Fig. 15 *b*). Although radiating actin bundles were heavily decorated with colloidal gold, the core region still remained unlabeled (*arrow*), suggesting inadequate penetration of gold particles into this highly condensed material (20). As far as we have examined, the actin bundles around the foci incorporated biotin-actin the slowest among the actin-containing structures within the injected cells.

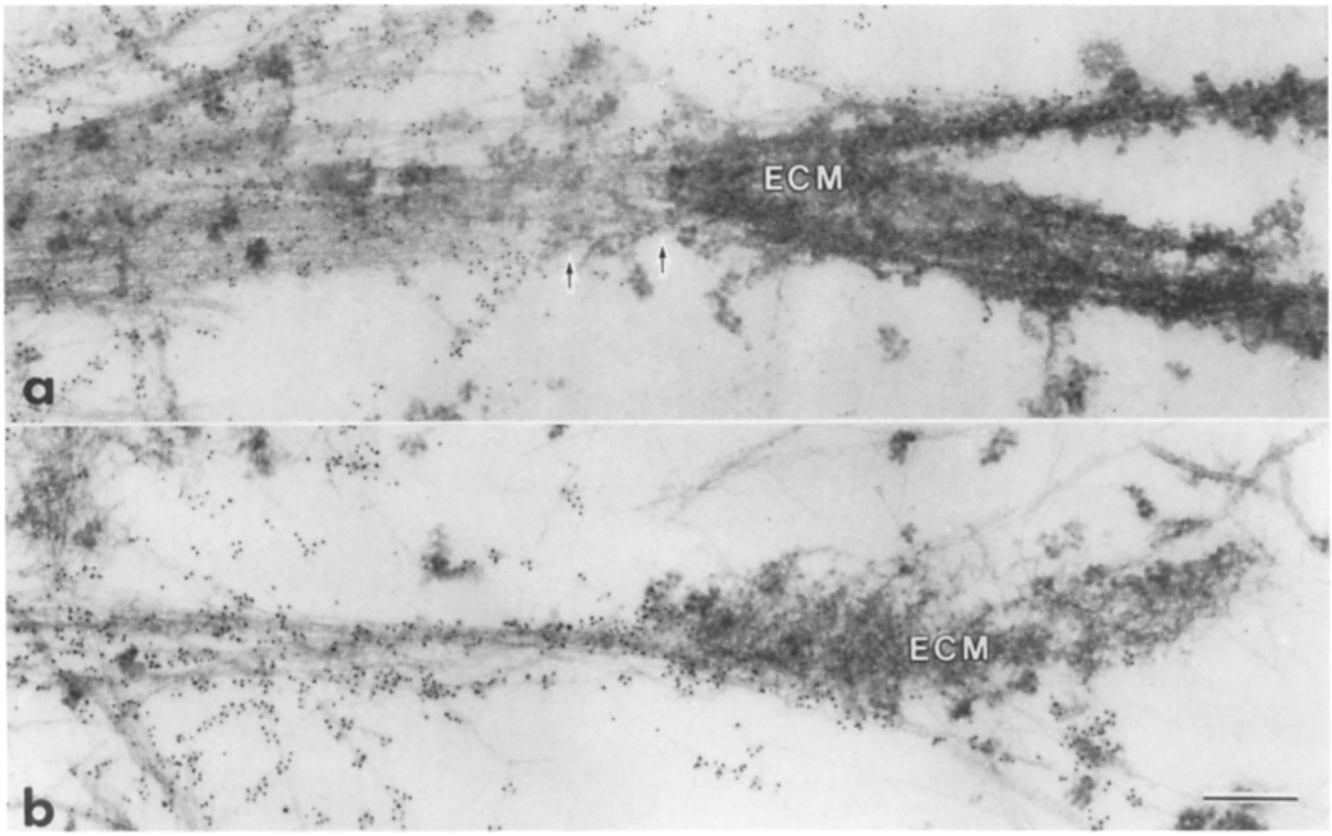

Figure 14. Electron micrographs of focal contacts within cells injected with biotin-actin. (*a*) A region of focal contacts in the cell permeabilized 2 min 32 s after injection. Actin filaments at focal contacts were largely unlabeled. (*b*) A region of focal contacts in the cell permeabilized 10 min after injection. Actin filaments have already incorporated biotin-actin prominently. *ECM*, extracellular matrix. Bar, 200 nm.

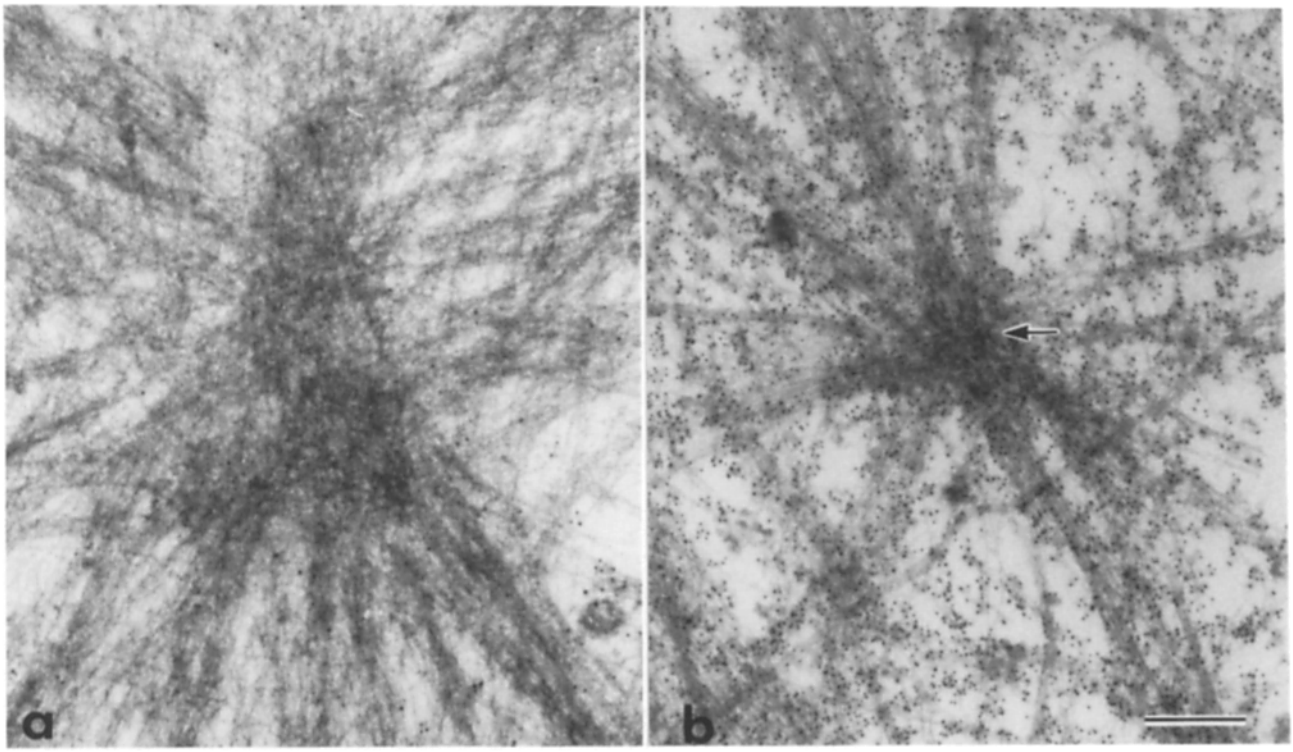

Figure 15. Electron micrographs of dense circular foci of polygonal nets within cells injected with biotin-actin. (*a*) A focus of a cell injected 2 min 32 s before permeabilization. Few gold particles were localized on the radiating actin bundles. (*b*) A focus of a cell incubated for 1 h after injection. The actin bundles of polygonal network were labeled prominently but the core region still remained unlabeled (*arrow*). Bar, 200 nm.

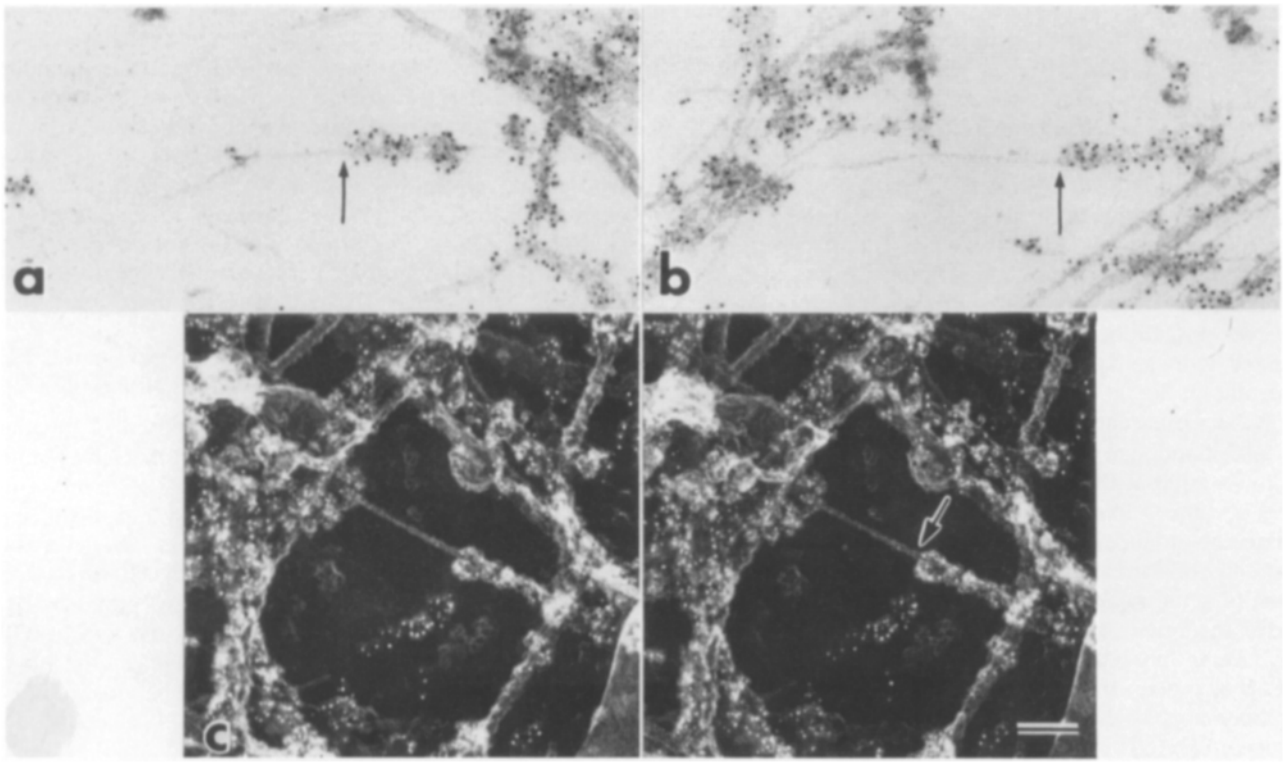

Figure 16. Electron micrographs of junctures between labeled and unlabeled segments of single actin filaments. In thin sections (*a* and *b*) and in freeze-dried samples (*c*) of the cytoskeleton of injected cells, junctures between labeled and unlabeled segments can be observed (*arrows*). Bar, 100 nm.

Turnover of Single Actin Filaments

In the cells that were fixed a few minutes after injection, we frequently observed actin segments that were fully decorated with colloidal gold and continuous to unlabeled segments (Fig. 16, *a* and *b*). These junctures between labeled and unlabeled segments could also be seen by freeze-drying techniques. Fig. 16 *c* shows a peripheral region of a cell permeabilized shortly (<5 min) after injection, and a juncture between heavily labeled and unlabeled segments of a single actin filament can be clearly observed. These results are consistent with previous in vitro data that have shown that actin filament assembly is mediated by the interaction of filament ends with actin monomers (15, 27). However, there remains another possibility that these junctures are the points where annealing of two filaments occurs (23).

Discussion

Experimental Design

In this study we followed the incorporation of microinjected biotin-actin into actin-containing cytoskeletal domains of fibroblastic cells. The major concern for microinjection experiments is the possibility that injection procedures disturb the steady state of actin filament dynamics. Using the method described in our previous paper (24), the injected volume per each cell was estimated to be <10% of the cell volume. Because cells were injected with biotin-actin at a concentration of 2 mg/ml and a concentration of actin within fibroblasts was reported to be 4 mg/ml (4), we estimated the increase of the total actin pool to be up to 5%. Whether this slight increase of actin concentration after injection induces artifactual polymerization is not clear. However, the pattern of biotin-actin incorporation was essentially identical with biotin-actin concentrations of 0.5–3 mg/ml (data not shown). Therefore it is less likely that the increase of actin concentration by injection significantly perturbs native actin turnover in vivo. Possible effects of biotinylation on the properties of actin molecules should also be a concern. Biotin-actin behaved in the same manner as native actin during assembly–disassembly cycles in vitro. Biotin-actin polymerized in vitro formed long, straight, 7-nm filaments. Furthermore, the pattern and rate of biotin-actin incorporation into the cytoskeleton was in good agreement with previous light microscopic studies (8, 16). These data collectively indicate that biotinylation does not affect assembly properties of actin.

Actin Dynamics in the Leading Lamella

Incorporation of injected actin into the leading edge occurs within 1 min after injection and this rapid incorporation is in agreement with previous reports (8, 16). Furthermore, we have illustrated that the incorporation of actin occurs at the distal part of actin bundles in microspikes and membrane-associated fringes of actin networks in lamellipodia. In microspikes, actin filaments form tightly packed bundles and are oriented with their barbed ends toward the cell periphery (32, 33). Therefore, incorporation of biotin-actin into the distal part of actin bundles suggests that the actin polymerization occurs at the barbed ends of preexisting filaments within microspikes. With longer incubation, biotin-actin is also incorporated into the membrane-associated surface region of actin bundles. One possible explanation of this label-

ing pattern is that the incorporation of biotin-actin occurs at the filament ends that are distributed along the surfaces of actin bundles within microspikes. Because microspikes have decreasing diameters and probably decreasing numbers of actin filaments toward their tips, it is likely that the ends of actin filaments are not restricted to the tips of microspikes but are distributed along their length. Another possibility is that actin filaments in the surface region extend along the entire length of microspikes and have their ends exclusively at the tips, but are more dynamic than filaments in the core region and turn over rapidly. Although it is difficult to discern these two possibilities from our observations, the results presented here clearly illustrate that the turnover of actin in microspikes is not uniform and the incorporation mainly occurs at the membrane-associated regions.

In lamellipodia, we also observed that the incorporation of actin is rapid at the membrane-associated peripheral regions. Because it has been documented previously that actin filaments in lamellipodia are largely oriented with their barbed ends toward the leading edge (32, 33), the observed pattern of actin incorporation may result from the addition of actin monomers at the barbed ends of preexisting filaments. Wang has reported a constant movement of rhodamine-labeled actin molecules toward the cell center within lamellipodia using the method of photobleaching by a laser microbeam (37). This result is in agreement with our observations because the movement of the bleached zone away from the cell periphery suggests continuous incorporation of actin monomer at the cell periphery. Our results have shown that the rate and pattern of actin incorporation into the cytoskeleton does not largely differ between microspikes and lamellipodia, suggesting that actin dynamics in these cellular regions are driven by a common underlying mechanism.

Actin Dynamics in Stress Fibers

Using fluorescently labeled actin analogues, several reports have illustrated that the turnover of actin in stress fibers is slower than that of the leading lamella (2, 8, 16, 17). However, precise description of the pattern of actin incorporation into stress fibers has not yet been obtained. We characterized the incorporation of actin into stress fibers on a molecular level by immunoelectron microscopy. Injected biotin-actin was first incorporated onto the surface of stress fibers and then gradually into the core region of fibers. These observations are in agreement with a previous report of Amato and Taylor (2) that has characterized the turnover of fluorescently labeled actin by immunoelectron microscopy. At 5–10 min after injection, increasing density of labeling along stress fibers was observed, and thinner bundles in peripheral cellular regions incorporated biotin-actin more rapidly than thicker bundles in the perinuclear region. It has been documented that terminal regions of stress fibers continue to be reorganized within living cells (36) and rapid turnover of actin in thin bundles would be partly due to de novo formation of stress fibers at motile peripheral regions.

Actin Dynamics at Focal Contacts

Focal contacts are sites of cell–substratum adhesion and also serve as attachment sites of stress fibers (6, 10). Although actin filaments in stress fibers have antiparallel polarities in general, those at focal contacts are oriented with their barbed ends toward the plasma membrane (29). These differences in the polarity orientation raise the possibility that dynamics of actin turnover at focal contacts differ from it in the other parts of stress fibers. However, our results have indicated that uniformly polarized microfilaments at focal contacts do not incorporate free monomers rapidly. This also suggests that turnover rate of actin filaments at the barbed ends differs between the leading edge and focal contacts (8). Because there are several proteins that are specifically localized at focal contacts, it is possible that these proteins regulate the dynamics of actin turnover locally through their interaction with filament ends (6).

Actin Dynamics in the Foci of Polygonal Network

Polygonal nets of actin bundles are composed of circular dense foci and interconnecting actin bundles that have a similar molecular composition to stress fibers (21, 28, 30). Our observations have indicated that the turnover of actin filaments in the polygonal nets is a slow process, and actin filaments in this region are stabilized by an unknown mechanism possibly with involvement of actin-binding proteins. Because Sanger et al. (30) have shown that the foci of 3T3 fibroblasts continue to subdivide and/or disappear, the incorporation of biotin-actin after extended incubation would be partly due to reorganization of actin filaments around the foci during these structural changes.

In conclusion, the data presented here illustrated differential patterns of actin turnover in four distinct cytoplasmic domains: the leading lamella, stress fibers, focal contacts, and circular dense foci. Motile behaviors of a variety of cell types appear to be closely linked to the dynamic reorganization of actin filaments. A better understanding of the mechanism of cellular motility will require further information about the molecular dynamics of the actin assembly and actin–myosin interactions. Further studies using the techniques of cryogenic sample preparation in combination with microinjection of cytoskeletal proteins will soon provide new information about this issue.

We thank Dr. H. Yoshikura (University of Tokyo, Tokyo, Japan) for his kind gift of mouse 3T3 fibroblasts and Dr. T. Sakurai (University of Tokyo) for his help in characterizing the in vitro properties of biotin-actin. We are also grateful to Ms. Y. Kawasaki for her technical assistance.

The present study was supported by grants-in-aid for scientific research and for special project research by the Ministry of Education, Science, and Culture of Japan and by the Muscular Dystrophy Association of America to N. Hirokawa.

Received for publication 11 April 1989 and in revised form 12 June 1989.

References

1. Abercrombie, M., J. E. M. Heaysman, and S. M. Pegrum. 1971. The locomotion of fibroblasts in culture. IV. Electron microscopy of the leading lamella. *Exp. Cell Res.* 67:359–367.
2. Amato, P. A., and D. L. Taylor. 1986. Probing the mechanism of incorporation of fluorescently labeled actin into stress fibers. *J. Cell Biol.* 102:1074–1084.
3. Bradford, M. M. 1976. A rapid and sensitive method for the quantitation of microgram quantities of protein utilizing the principle of protein-dye binding. *Anal. Biochem.* 72:248–254.
4. Bray, D., and C. Thomas. 1975. The actin content of fibroblasts. *Biochem. J.* 147:221–228.
5. Bray, D., and J. G. White. 1988. Cortical flow in animal cells. *Science (Wash. DC).* 239:883–888.
6. Burridge, K., L. Molony, and T. Kelly. 1987. Adhesion plaques: sites of transmembrane interaction between the extracellular matrix and the actin

cytoskeleton. *J. Cell Sci. Suppl.* 8:211–229.
7. Forscher, P., and S. J. Smith. 1988. Actions of cytochalasins on the organization of actin filaments and microtubules in a neuronal growth cone. *J. Cell Biol.* 107:1505–1516.
8. Glacy, S. D. 1983. Subcellular distribution of rhodamine-actin microinjected into living fibroblastic cells. *J. Cell Biol.* 97:1207–1213.
9. Graessmann, A., M. Graessmann, and C. Mueller. 1980. Microinjection of early SV40 DNA fragments and T antigen. *Methods Enzymol.* 65:816–825.
10. Heath, J. P., and G. A. Dunn. 1978. Cell to substratum contacts of chick fibroblasts and their relation to the microfilament system: a correlated interference-reflexion and high-voltage electron-microscope study. *J. Cell Sci.* 29:197–212.
11. Heuser, J. E., and M. W. Kirschner. 1980. Filament organization revealed in platinum replicas of freeze-dried cytoskeletons. *J. Cell Biol.* 86: 212–234.
12. Hirokawa, N. 1986. Quick-freeze, deep-etch of the cytoskeleton. *Methods Enzymol.* 134:598–612.
13. Hirokawa, N., and J. E. Heuser. 1981. Quick-freeze, deep-etch visualization of the cytoskeleton beneath surface differentiations of epithelial cells. *J. Cell Biol.* 91:339–409.
14. Hirokawa, N., L. G. Tilney, K. Fujiwara, and J. E. Heuser. 1982. The organization of actin, myosin, and intermediate filaments in the brush border of intestinal epithelial cells. *J. Cell Biol.* 94:425–443.
15. Korn, E. D. 1982. Actin polymerization and its regulation by proteins from non-muscle cells. *Physiol. Rev.* 62:672–737.
16. Kreis, T. E., K. H. Winterhalter, and W. Birchmeier. 1979. In vivo distribution and turnover of fluorescently labeled actin microinjected into human fibroblasts. *Proc. Natl. Acad. Sci. USA.* 76:3814–3818.
17. Kreis, T. E., B. Geiger, and J. Schlessinger. 1982. Mobility of microinjected rhodamine actin within living chicken gizzard cells determined by fluorescence photobleaching recovery. *Cell.* 29:835–845.
18. Kristofferson, D., T. Mitchison, and M. Kirschner. 1986. Direct observation of steady-state microtubule dynamics. *J. Cell Biol.* 102:1007–1019.
19. Laemmli, U. K. 1970. Cleavage of structural proteins during the assembly of the head of bacteriophage T_4. *Nature (Lond.).* 227:680–685.
20. Langanger, G., J. De May, M. Moeremans, G. Daneels, M. D. Brabander, and J. V. Small. 1984. Ultrastructural localization of α-actinin and filamin in cultured cells with the immunogold staining (IGS) method. *J. Cell Biol.* 99:1324–1334.
21. Lazarides, E. 1976. Actin, α-actinin, and tropomyosin interaction in the structural organization of actin filaments in nonmuscle cells. *J. Cell Biol.* 68:202–219.
22. Mooseker, M. S., T. D. Pollard, and K. A. Wharton. 1982. nucleated polymerization of actin from the membrane-associated ends of microvillar filaments in the intestinal brush border. *J. Cell Biol.* 95:223–233.
23. Murphy, D. B., R. D. Gray, W. A. Grasser, and T. D. Pollard. 1988. Direct demonstration of actin filaments annealing in vitro. *J. Cell Biol.* 106:1947–1954.
24. Okabe, S., and N. Hirokawa. 1988. Microtubule dynamics in nerve cells: analysis using microinjection of biotinylated tubulin into PC12 cells. *J. Cell Biol.* 107:651–664.
25. Okabe, S., and N. Hirokawa. 1989. Rapid turnover of microtubule-associated protein MAP2 in the axon revealed by microinjection of biotinylated MAP2 into cultured neurons. *Proc. Natl. Acad. Sci. USA.* 86:4127–4131.
26. Pardee, J. D., and J. A. Spudich. 1982. Purification of muscle actin. *Methods Enzymol.* 85:164–181.
27. Pollard, T. D., and J. A. Cooper. 1986. Actin and actin-binding proteins: a critical evaluation of mechanisms and functions. *Annu. Rev. Biochem.* 55:987–1035.
28. Rathke, P. C., M. Osborn, and K. Weber. 1979. Immunological and ultrastructural characterization of microfilament bundles: polygonal nets and stress fibers in an established cell line. *Eur. J. Cell Biol.* 19:40–48.
29. Sanger, J. M., and J. W. Sanger. 1980. Banding and polarity of actin filaments in interphase and cleaving cells. *J. Cell Biol.* 86:568–575.
30. Sanger, J. M., B. Mittal, M. Pochapin, and J. W. Sanger. 1986. Observation of microfilament bundles in living cells microinjected with fluorescently labeled contractile proteins. *J. Cell Sci. Suppl.* 5:17–44.
31. Schliwa, M., and J. V. Blerkom. 1981. Structural interaction of cytoskeletal components. *J. Cell Biol.* 90:222–235.
32. Small, J. V., G. Isenberg, and J. E. Celis. 1978. Polarity of actin at the leading edge of cultured cells. *Nature (Lond.).* 272:638–639.
33. Small, J. V., G. Rinnerthaler, and H. Hinssen. 1982. Organization of actin meshworks in cultured cells: the leading edge. *Cold Spring Harbor Symp. Quant. Biol.* 46:559–612.
34. Tatjana, M. S., A. A. Neyfakh, and A. Bershadsky. 1986. Actin cytoskeleton of spread fibroblasts appears to assemble at the cell edge. *J. Cell Sci.* 82:235–248.
35. Tilney, L. G., and S. Inoue. 1982. Acrosomal reaction of thyone sperm. II. The kinetics and possible mechanism of acrosomal process elongation. *J. Cell Biol.* 93:820–827.
36. Wang, Y. -L. 1984. Reorganization of actin filament bundles in living fibroblasts. *J. Cell Biol.* 99:1478–1485.
37. Wang, Y. -L. 1985. Exchange of actin subunits at the leading edge of living fibroblasts: possible role of treadmilling. *J. Cell Biol.* 101:597–602.